Supplementary Information

Role of the donor on the light-induced degradation of Y6 non-fullerene acceptors in PM6:Y6 blend films

Suraj Prasad, C. Moyses Araujo, Ellen Moons*

Department of Engineering and Physics, Karlstad University, SE-65188 Karlstad, Sweden.

* Corresponding author (e-mail: ellen.moons@kau.se)

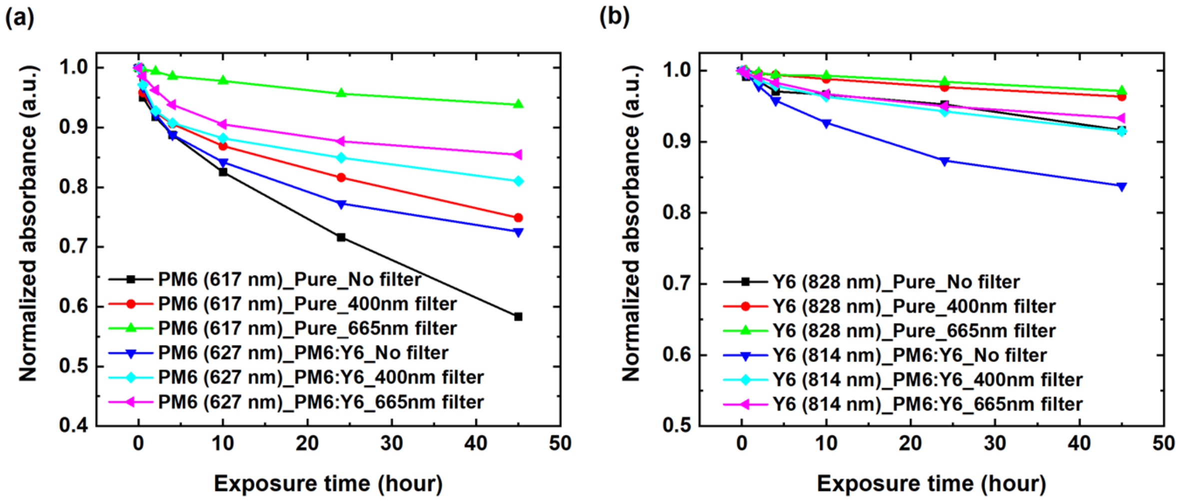

Figure S1: The relative change in absorbance at specific wavelengths, extracted from the UV-vis spectra of PM6, Y6, and PM6:Y6 films exposed for 0 min, 30 min, 2 h, 4 h, 10 h, 24 h, and 45 h in ambient conditions to AM1.5 light, with no filter, 400 nm, and 665 nm long-pass filters.

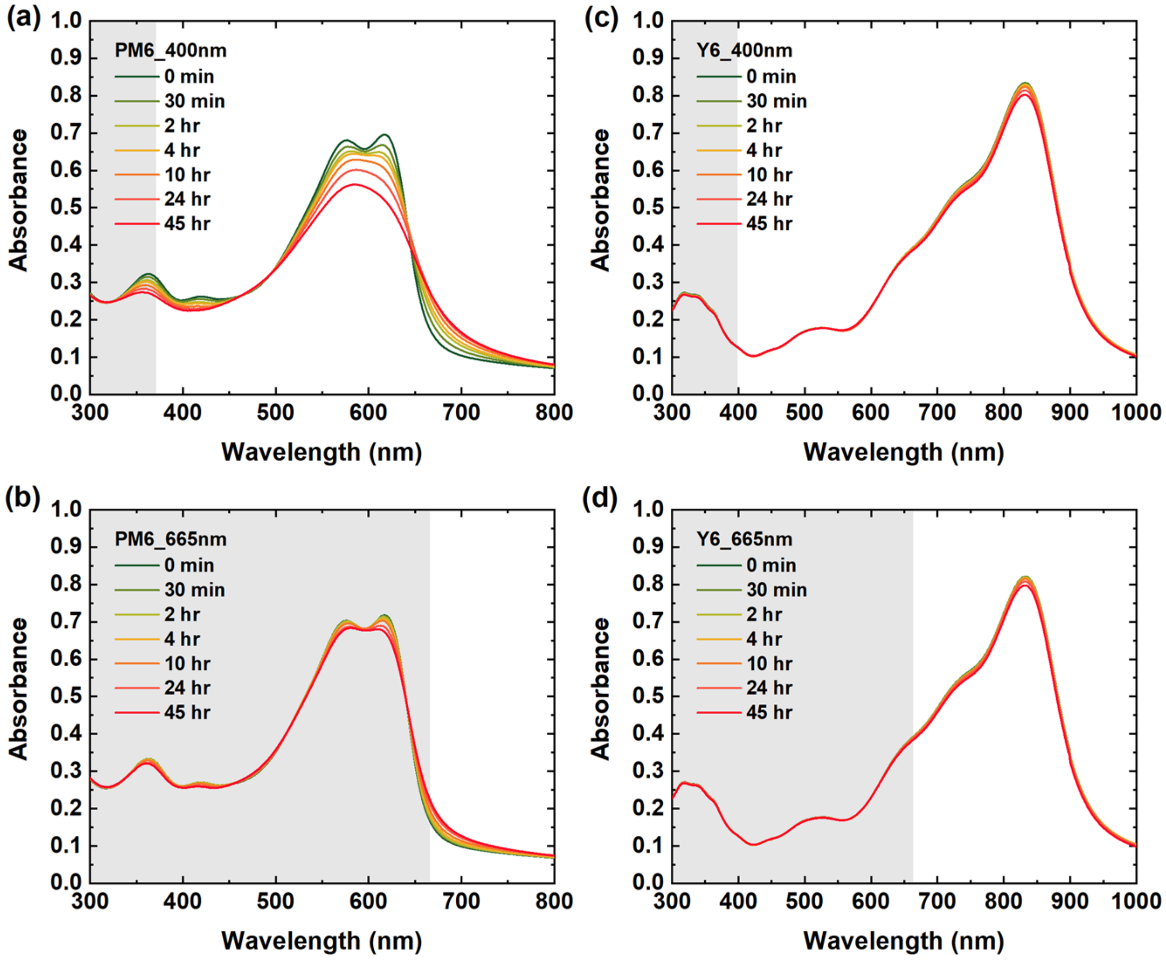

Figure S2: The optical absorption spectra of spin-coated films (a, b) PM6 and (c, d) Y6 measured in air before and after photodegradation by exposure for different times (30 min, 2 h, 10 h, 24 h, and 45 h) to AM1.5 light in air with LP400 and with LP665 filters.

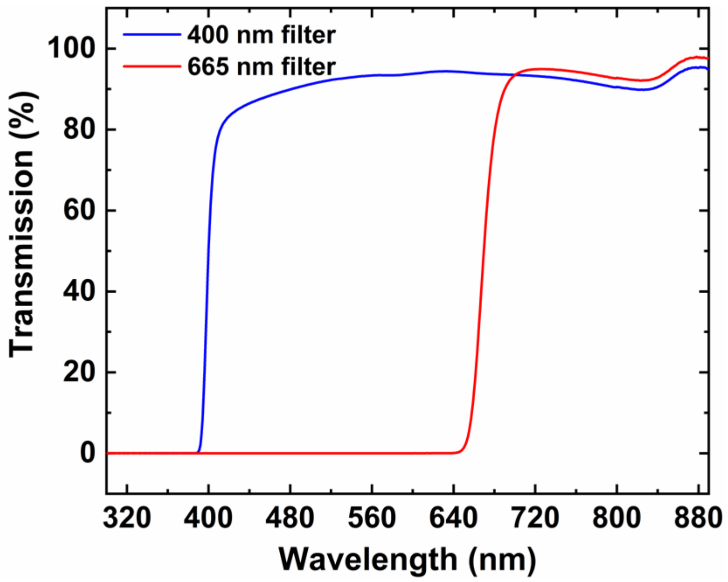

Figure S3: The transmission spectra of the 400 nm and 665 nm long pass filters used for the degradation experiments.

Table S1: Position and assignment of the IR absorption peak of unexposed PM6 from Figure S4.

Peak index	Frequency (cm^{-1})	Assignment	Ref.
1	1100-1400	C-H rocking and scissoring modes	[1-4]
2	1455	CH_2 bending mode	[1-4]
3	1474	CH_2 bending mode	[1-4]
4	1518	CH_2 bending mode	[1-4]
5	1649	C=O stretch (quinone group)	[1,5-7]

Table S2: Position and assignment of the IR absorption peak of unexposed Y6 from Figure S4.

Peak index	Frequency (cm^{-1})	Assignment	Ref.
1	1230	CH and CH_2 rocking modes	[3,8]
2	1253	CH and CH_2 rocking modes	[3,8]
3	1290	CH and CH_2 rocking modes	[3,8]
4	1426	C=C stretch modes (conjugate plane)	[4]
5	1506	C=C stretch modes (thiophene)	[4]
6	1535	malononitrile moieties dominated by C-C mode	[9]
7	1600	C=N stretch	[4,8]
8	1697	C=O stretch from the five-membered carbon ring	[1,4,5]
9	2216	C≡N stretch	[1,4,8]

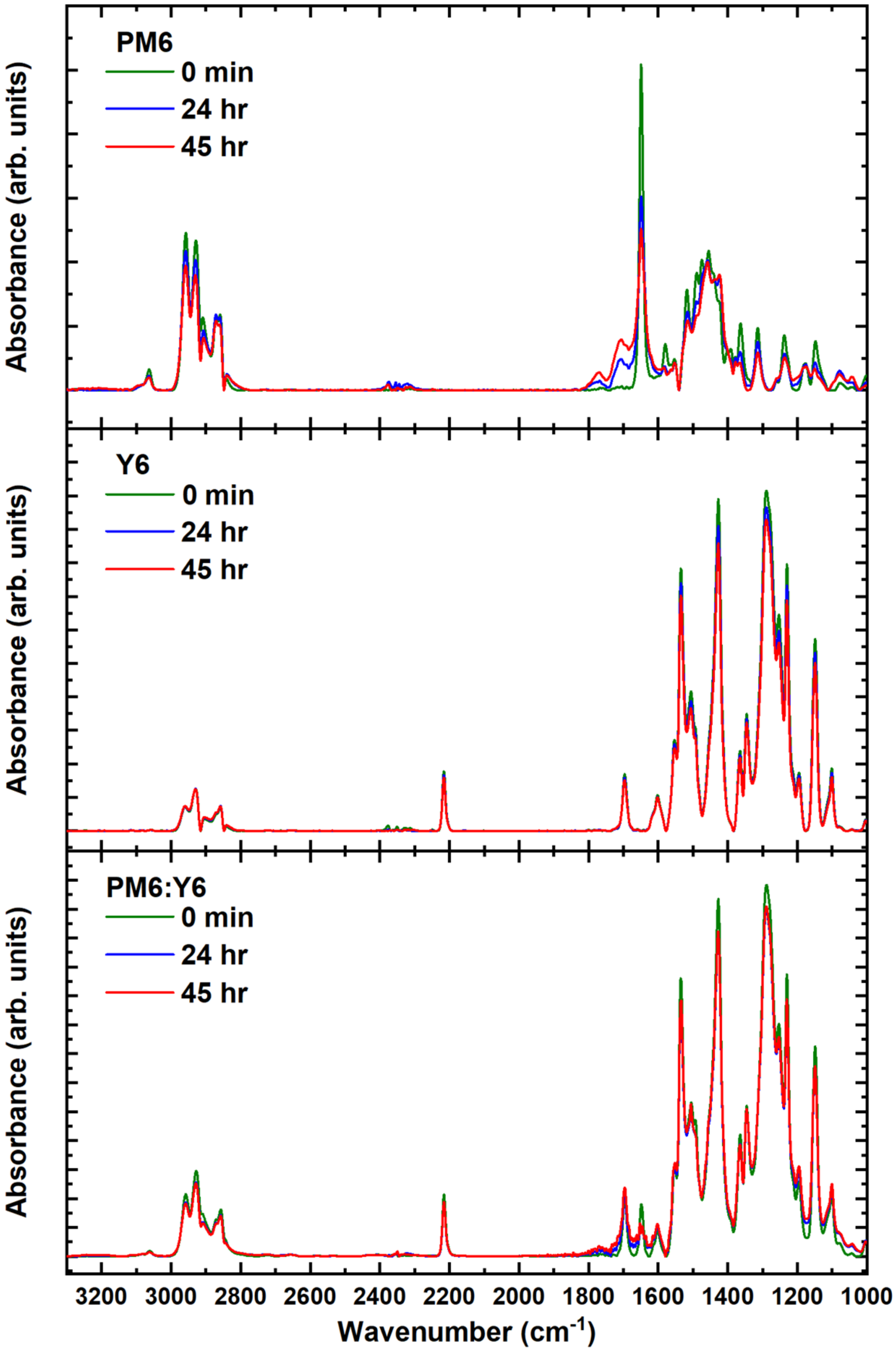

Figure S4: The wide range FTIR spectra, measured in transmission mode, of spin-coated films of pristine PM6 (top), Y6 (middle), and PM6:Y6 (1:1) (bottom) on KBr, unexposed and exposed in the air to white light (AM 1.5) for 24 h and 45 h.

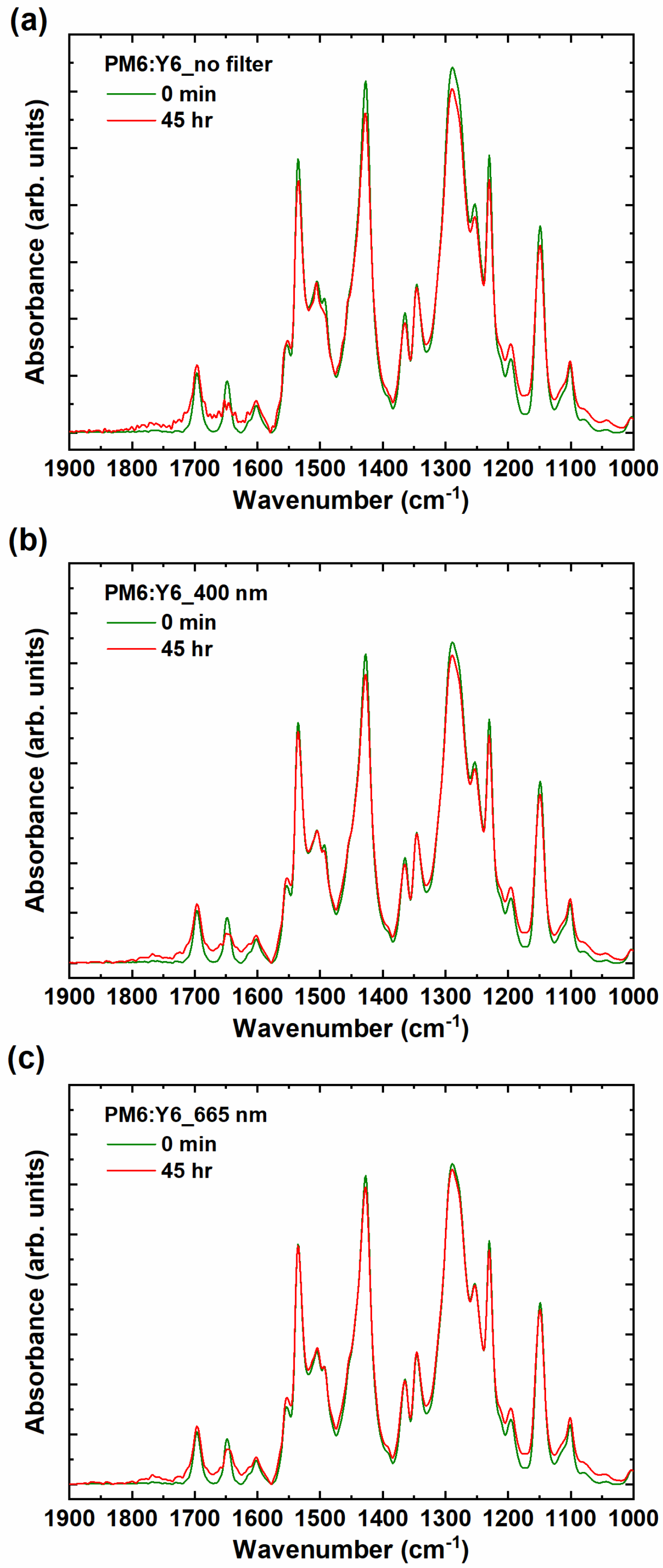

Figure S5: The FTIR spectra of pristine PM6:Y6 unexposed and exposed under AM 1.5 for 45 h in the presence of no filter (a), 400 nm (b), or 665 nm (c) long-pass filter conditions.

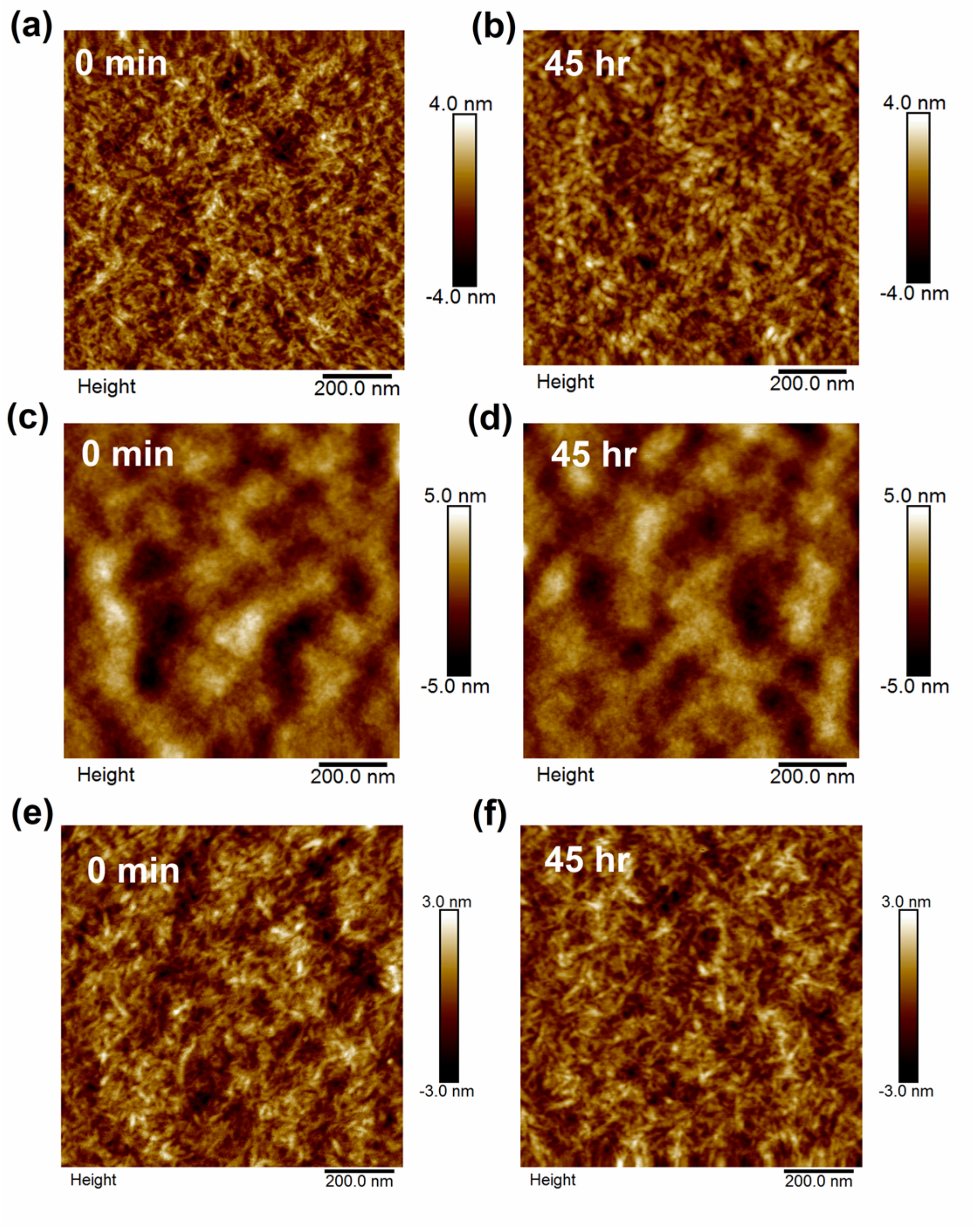

Figure S6: AFM height images of PM6 (a,b), Y6 (c,d), and PM6:Y6 (e,f) for unexposed (0 min) and exposed in the air to white light (AM 1.5) for 45 h.

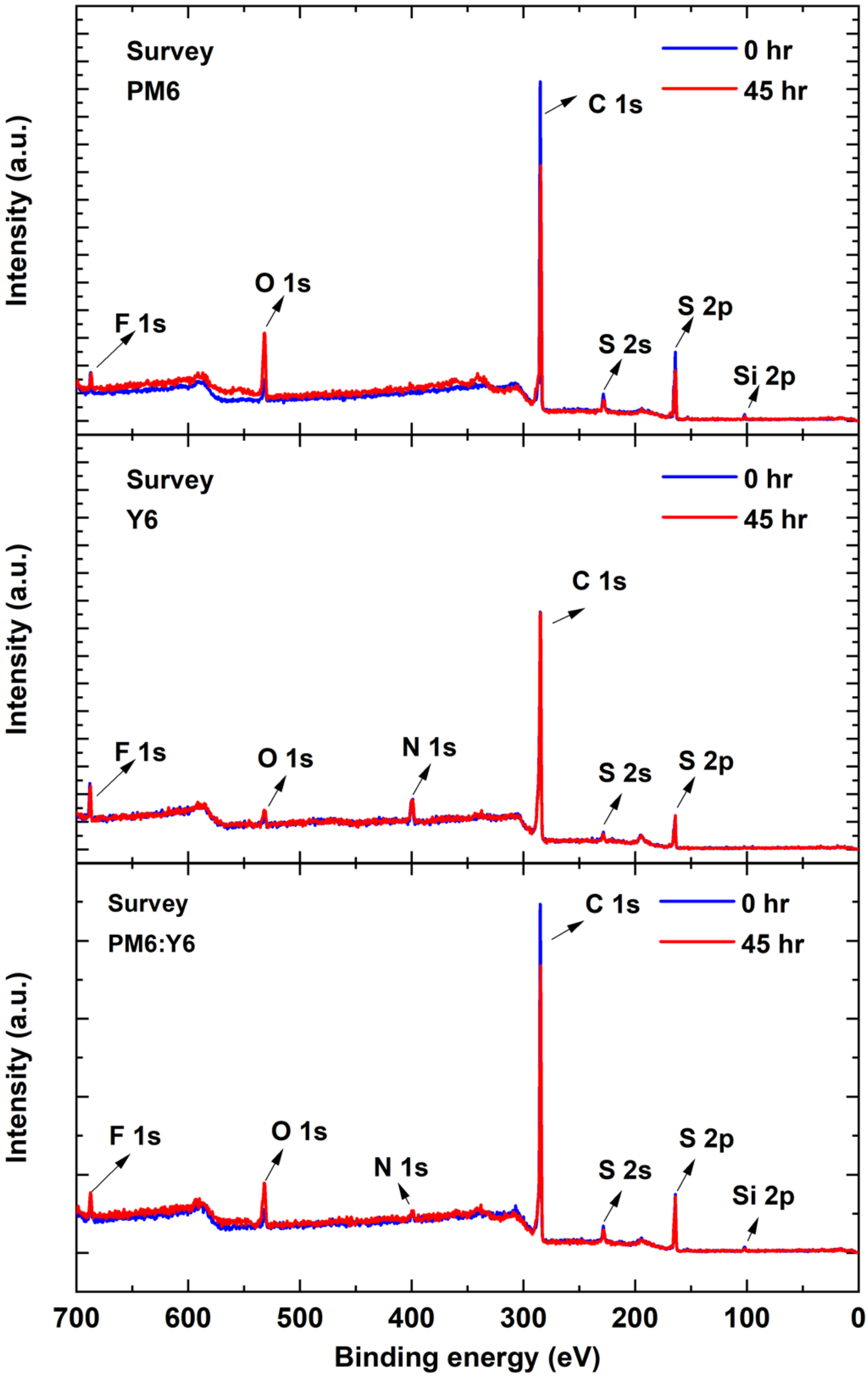

Figure S7: The high-resolution XPS spectra of PM6 (top), Y6 (middle), and PM6:Y6 (bottom) of unexposed (0 h) and exposed in the air to white light (AM 1.5) for 45 h.

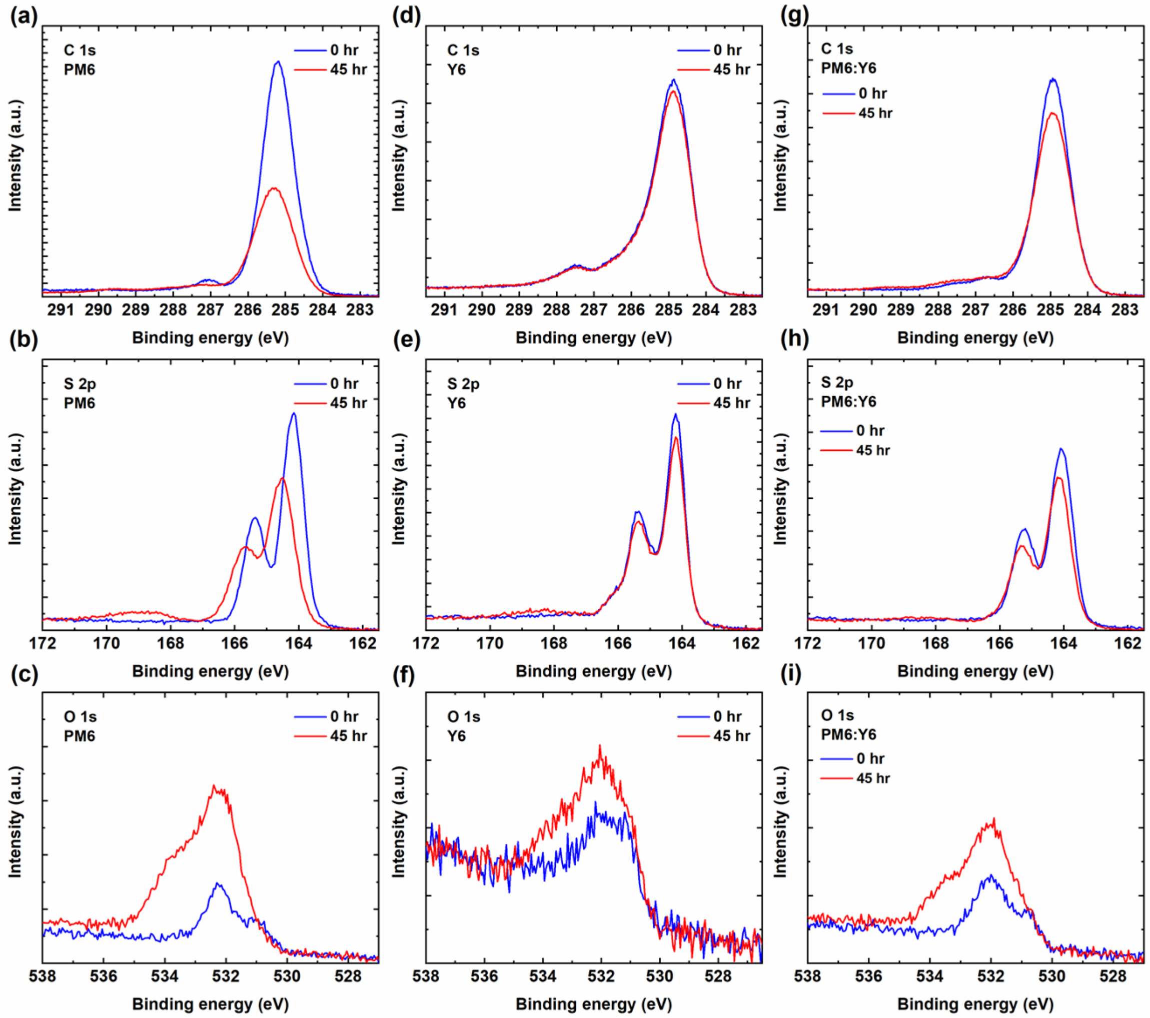

Figure S8: XPS core level spectra of PM6 (left), Y6 (middle), and PM6:Y6 (right) for unexposed and exposed in the air to white light (AM 1.5) for 45 h in ambient conditions of C 1s, S 2p, and O 1s.

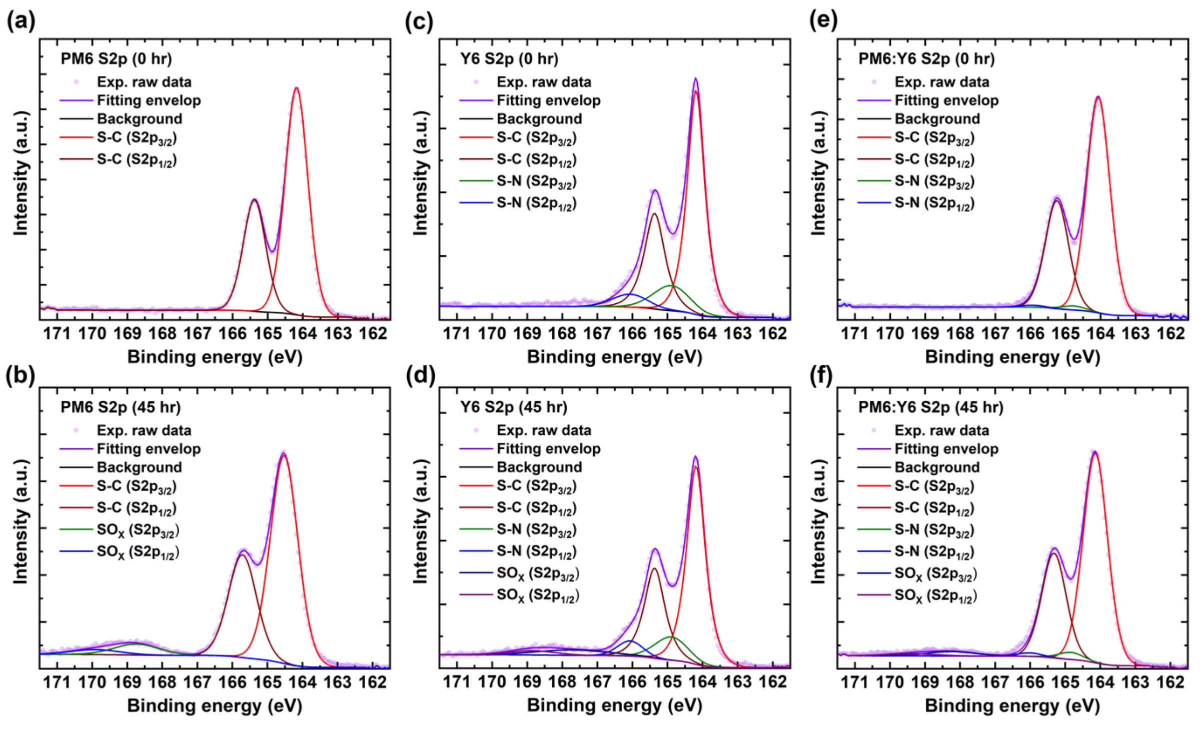

Figure S9: High-resolution XPS S 2p core level spectra of PM6 (left), Y6 (middle), and the PM6:Y6 blend (right) films. Spectra are presented for fresh samples (0 h) (top row) and after 45 h of degradation under AM 1.5 illumination in air (bottom row), as indicated in the legends.

The core level S 2p spectra of PM6, presented in Figure S9a, show a doublet S $2p_{1/2}$ and S $2p_{3/2}$, at 165.38 eV and 164.18 eV, respectively, corresponding to the sulfur C-S bonds. After 45 h of photooxidation (Figure S9b), the intensities of the peaks corresponding to S $2p_{1/2}$ and S $2p_{3/2}$ decrease and shift toward higher binding energies, now appearing at 165.71 eV and 164.52 eV (see Figure S8b). Additionally, new peaks emerge at higher binding energies. The shift toward higher binding energy suggests that the S core level electrons become more tightly bound, while the appearance of the new peaks indicates the formation of oxidized sulfur species (SO_x). Figure S9c shows the core level S 2p spectra of the Y6 for the unexposed sample. The doublets S $2p_{1/2}$ and S $2p_{3/2}$ are observed at 165.37 eV and 164.19 eV, corresponding to the sulfur core levels of C-S. Another set of doublets at 166.07 eV and 164.89 eV corresponds to the sulfur core levels of the C-N. After 45 h of photooxidation (Figure S9d), the intensities of these peaks show a minor decrease, and a new doublet appears at 168.87 eV and 167.69 eV (see Figure S7e). This new doublet likely indicates the formation of oxidized sulfur species in Y6. Similar behavior has been previously reported for the Y5 and Y6 acceptor.[1,9] Figure S9e shows the S 2p spectra of the PM6:Y6 blend at 0 h. As expected, the spectra reflect a combination of peaks from both PM6 (donor) and Y6 (acceptor). The S 2p doublets at 165.24 eV and 164.06 eV for the sulfur C-S bond, and at 165.94 eV and 164.76 eV for the sulfur C-N core levels from Y6. After 45 h of photooxidation (Figure S9f), the C-S related peaks shift slightly to higher binding energies (165.32 eV), and their intensities decrease (see Figure S8h). Similarly, the S-N related peaks shift to 166.02 eV. A new set of peaks appears at higher binding energy, indicating the formation of oxidized sulfur species.

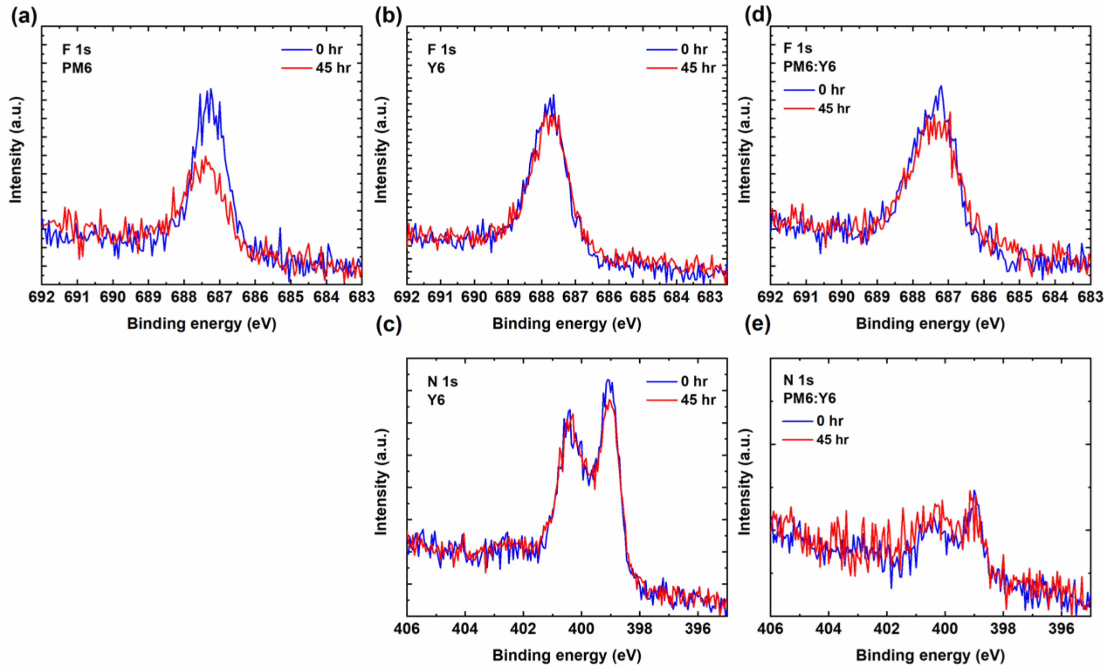

Figure S10: XPS core level spectra of PM6 (left), Y6 (middle), and PM6:Y6 (right) for unexposed and exposed in the air to white light (AM 1.5) for 45 h in ambient conditions of F 1s and N1s.

References

1 S. Prasad, Z. Genene, C. F. N. Marchiori, S. Singh, L. K. E. Ericsson, E. Wang, C. M. Araujo & E. Moons. Effect of molecular structure on the photochemical stability of acceptor and donor polymers used in organic solar cells. *Materials Advances* (2024).

2 Y. Wang, J. Luke, A. Privitera, N. Rolland, C. Labanti, G. Londi, V. Lemaur, D. T. W. Toolan, A. J. Sneyd, S. Jeong, D. Qian, Y. Olivier, L. Sorace, J.-S. Kim, D. Beljonne, Z. Li & A. J. Gillett. The critical role of the donor polymer in the stability of high-performance non-fullerene acceptor organic solar cells. *Joule* **7**, 810-829 (2023).

3 J. Guo, Y. Wu, R. Sun, W. Wang, J. Guo, Q. Wu, X. Tang, C. Sun, Z. Luo, K. Chang, Z. Zhang, J. Yuan, T. Li, W. Tang, E. Zhou, Z. Xiao, L. Ding, Y. Zou, X. Zhan, C. Yang, Z. Li, C. J. Brabec, Y. Li & J. Min. Suppressing photo-oxidation of non-fullerene acceptors and their blends in organic solar cells by exploring material design and employing friendly stabilizers. *Journal of Materials Chemistry A* **7**, 25088-25101 (2019).

4 J. Coates. Interpretation of infrared spectra, a practical approach. *Encyclopedia of analytical chemistry* **12**, 10815-10837 (2000).

5 T. Shan, Y. Zhang, Y. Wang, Z. Xie, Q. Wei, J. Xu, M. Zhang, C. Wang, Q. Bao, X. Wang, C.-C. Chen, J. Huang, Q. Chen, F. Liu, L. Chen & H. Zhong. Universal and versatile morphology engineering via hot fluorous solvent soaking for organic bulk heterojunction. *Nature Communications* **11**, 5585 (2020).

6 X. Wei, L. Jia, B. Duan, X. Wang, L. Du, S. Li, Z. Xu & W. Zhao. Recent Progress and Applications of NanoIR-AFM in Morphological Characterization of Organic Solar Cells. *Advanced Functional Materials* **34**, 2408960 (2024).

7 S. H. K. Paleti, S. Hultmark, J. Han, Y. Wen, H. Xu, S. Chen, E. Järsvall, I. Jalan, D. R. Villalva, A. Sharma, J. I. Khan, E. Moons, R. Li, L. Yu, J. Gorenflot, F. Laquai, C. Müller & D. Baran. Hexanary blends: a strategy towards thermally stable organic photovoltaics. *Nature Communications* **14**, 4608 (2023).

8 J. Zhang, J. Guan, Y. Zhang, S. Qin, Q. Zhu, X. Kong, Q. Ma, X. Li, L. Meng, Y. Yi, J. Zheng & Y. Li. Direct Observation of Increased Free Carrier Generation Owing to Reduced Exciton Binding Energies in Polymerized Small-Molecule Acceptors. *The Journal of Physical Chemistry Letters* **13**, 8816-8824 (2022).

9 Q. Zhang, Y. Chen, X. Liu & M. Fahlman. In situ near-ambient pressure X-ray photoelectron spectroscopy reveals the effects of water, oxygen and light on the stability of PM6:Y6 photoactive layers. *Journal of Materials Chemistry C* **11**, 3112-3118 (2023).